

# Effect of ionic interaction on elongational viscosity of ethylene-based ionomer melts

Tatsuhiro Takahashi, Jun Watanabe, Keiji Minagawa and Kiyohito Koyama\*

Department of Materials Science and Engineering, Yamagata University, Yonezawa 992, Japan

(Received 17 March 1994; revised 2 May 1994)

The effects of ionic interaction on the uniaxial extensional flow of polymer melts were investigated using poly(ethylene-co-methacrylic acid) and its metal (Zn, Na, Mg) salts. The presence of ionic bonding enhanced the elongational viscosity in the linear region and the degree of non-linearity. Both the linear and non-linear elongational viscosities were increased more by zinc ions than by sodium or magnesium ions. The order of elongational viscosities was in agreement with the order of activation energies obtained from dynamic shear measurements. It was concluded that the increase in both linear elongational viscosity and non-linearity is determined by the degree of ionic interaction. The different flow properties between zinc and magnesium ionomers indicated that the ionic cluster formation weakens the ionic interaction. A Bernstein-Kearsley-Zapas constitutive analysis revealed that the effect of ionic interaction under elongational deformation in the linear region is similar to that under dynamic shear deformation.

(Keywords: elongational viscosity; ionomer; ionic interaction)

## INTRODUCTION

Investigation of the uniaxial elongational viscosity is important for understanding polymer processing since the elongational deformation is dominant in blow moulding, film moulding and melt spinning. A number of experimental studies<sup>1-15</sup> on the elongational flow of polymer melts have been made to clarify the effects of molecular parameters such as molecular weight, molecular weight distribution (*MWD*) and long-chain branching. The effects of experimental conditions, for example constant strain rate, constant stress and temperature, have also been examined. Elongational viscosities have been investigated for homogeneous polymers such as polystyrenes<sup>1-3</sup>, polyethylenes (high density polyethylene<sup>4</sup>, linear low density polyethylene<sup>5,6</sup> and low density polyethylene<sup>7-13</sup>), polypropylene<sup>14</sup> and polybutene-1<sup>15</sup>. The elongational viscosity as a function of time can be divided into two regions: the first region corresponds to a gradual viscosity increase, i.e. the linear region, and this is followed by a rapid viscosity increase, i.e. the non-linear region. The non-linearity parameter is defined as the non-linear viscosity divided by the linear viscosity<sup>14</sup>. The dependences of non-linearity on strain rate and temperature are strong for polystyrenes with narrow *MWDs*, while the dependences are weaker for polymers with wide *MWDs*<sup>1-3</sup>. On the other hand, the degree of non-linearity is enhanced by the existence of long-chain branching and a very high molecular weight<sup>4-13</sup>.

The presence of ionic bonding has a significant effect on the flow properties of ionomer melts. Experimental

studies on the shear viscoelastic properties of ionomer melts have been reported<sup>16-20</sup>. Shohamy and Eisenberg investigated the dynamic shear viscosities of poly(styrene-co-methacrylic acid), its ester and its sodium salt<sup>17</sup>. Their results revealed that the time-temperature superposition principle is applicable to the three samples, and that the shapes of the  $G'$  curves among the three samples are identical. Earnest and MacKnight evaluated the effect of hydrogen bonding and ionic interaction on the dynamic shear properties of poly(ethylene-co-methacrylic acid) (E/MAA), its methyl ester and its sodium salt<sup>18</sup>. They also found that the superposition of  $G'$  among the three samples is applicable with horizontal shifting. On the other hand, studies on the elongational viscosity of ionomers are few. Connelly *et al.* reported that the viscoelastic properties of polyester ionomers are less influenced by ionic interaction under extensional deformation than under steady shear deformation<sup>21</sup>. Further studies are needed to clarify the effect of ionic interaction under elongational deformation.

Constitutive analysis provides us with additional information about the rheological properties of polymer melts<sup>22-27</sup>. For example, the strain rate independent non-linearity of low density polyethylene (LDPE) is explained by a very long time relaxation mode in addition to the usual relaxation spectrum predicted by the Lodge model<sup>12</sup>. The Bernstein-Kearsley-Zapas (BKZ) model is known to be an excellent approximation equation for polymer melts<sup>22,26</sup>. The memory function of the BKZ equation is experimentally separated into two functions: the time dependent function  $\mu(t-t')$  and the strain dependent function  $h(I, II)$ <sup>28,29</sup>. The Doi-Edwards theory<sup>30</sup> supports this separability. Recently, we have found that

\* To whom correspondence should be addressed

the time-strain factorization is applicable to E/MAA and its metal salts in shear stress relaxation experiments<sup>31</sup>. Hence, we used the BKZ constitutive equation to analyse the effect of ionic interaction on elongational viscosity.

This work presents the elongational viscosities of E/MAA and its metal (Zn, Na, Mg) salts as a function of time at constant strain rate to clarify the effect of ionic interaction under elongational flow. The elongational viscosity in both the linear and non-linear regions is analysed using the BKZ equation and the corresponding relaxation spectrum. The role of ionic interaction in ionomer melts and the effect of ionic species on elongational viscosity are discussed.

## EXPERIMENTAL

Poly(ethylene-co-methacrylic acid) (E/MAA,  $M_n = 19\,200$ ,  $M_w = 94\,500$ ) with a methacrylic acid content of 15.0 wt% was used. The ethylene-based ionomers were E/MAA neutralized partially by zinc, sodium or magnesium ions, i.e. 59% Zn, 54% Na or 60% Mg. These are designated as E/MAA 0.59Zn, E/MAA 0.54Na and E/MAA 0.60Mg, respectively. All of these samples were kindly provided by Mitsui-DuPont Polychemicals. The melting temperature was 90°C for each sample.

Experiments on oscillatory shear were conducted using a rotational rheometer (Rheometrics RMS800) at 140°C, 170°C and 200°C. The test fixtures were parallel discs with a diameter of 25 mm for E/MAA and 8 mm for its metal salts. The input strain was sufficiently small to provide reliable linear viscoelastic data. All pellet samples were pretreated in a vacuum oven at 60°C for three days to eliminate water before measurements.

The elongational viscosity measurements were performed using our own Meissner-type rheometer. The reliability of the experimental apparatus has been described in an earlier paper<sup>14</sup>. Rod-like samples were produced with a single-screw extruder through a die. The sample diameter and length were about 5 mm and 30 cm, respectively. The samples were dried in a vacuum oven at 60°C for three days before testing. The rod-like samples were immersed in a silicone oil bath heated at 140°C. Since the rod-like samples shrank slightly on heating, 10 min of equilibration time were allowed before experiments. The molten samples were elongated at constant strain rate by rotating a pair of gears. The homogeneity of the elongational deformation was checked using a video camera, and the actual strain rate was calculated from the decrease in rod diameter. The setting strain rates used were in the range 0.005–0.5 s<sup>-1</sup>.

## RESULTS AND DISCUSSION

Dynamic shear measurements on E/MAA, E/MAA 0.59Zn, E/MAA 0.54Na and E/MAA 0.60Mg were carried out at 140°C, 170°C and 200°C. The storage modulus  $G'$  and loss modulus  $G''$  were obtained as a function of angular frequency ( $\omega$ ) in the range 0.1–100 rad s<sup>-1</sup>. The resulting  $G'$  and  $G''$  curves were shifted with respect to the curves at 170°C. Figure 1 shows that the time-temperature superposition principle is applicable to E/MAA 0.60Mg under the measurement conditions employed. The superposition principle was also applicable to E/MAA, E/MAA 0.59Zn and E/MAA

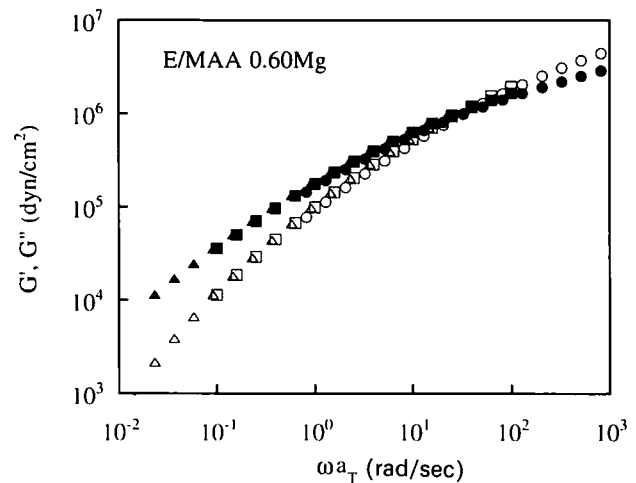


**Figure 1** Master curves of  $G'$  (open symbols) and  $G''$  (closed symbols) for E/MAA 0.60Mg measured at various temperatures (1 dyn = 10<sup>-5</sup> N): (○, ●) 140°C; (□, ■) 170°C; (△, ▲) 200°C. The reference temperature was 170°C

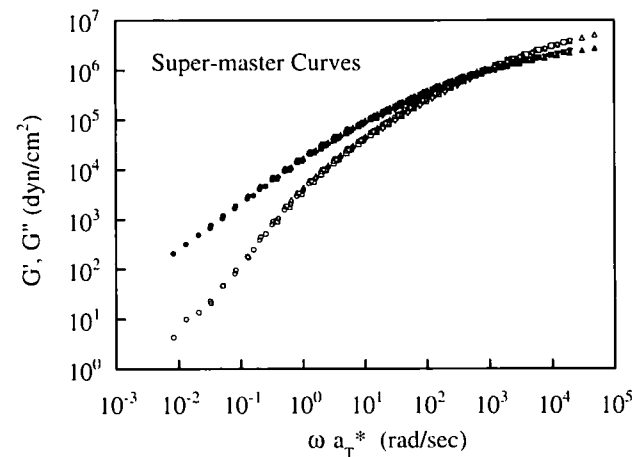


**Figure 2** Super-master curves of  $G'$  (open symbols) and  $G''$  (closed symbols) from master curves of E/MAA (○, ●), E/MAA 0.59Zn (□, ■), E/MAA 0.54Na (△, ▲) and E/MAA 0.60Mg (▽, ▼). The reference curve was for E/MAA at 140°C

0.54Na. The horizontal shift factors ( $a_T$ ) were estimated from superposition of the  $G'$  and  $G''$  curves, and they followed the Arrhenius equation. The activation energies for E/MAA, E/MAA 0.59Zn, E/MAA 0.54Na and E/MAA 0.60Mg were evaluated as 18.6 kcal mol<sup>-1</sup> K<sup>-1</sup>, 27.1 kcal mol<sup>-1</sup> K<sup>-1</sup>, 23.7 kcal mol<sup>-1</sup> K<sup>-1</sup> and 22.7 kcal mol<sup>-1</sup> K<sup>-1</sup>, respectively. The flow activation energy suggested that the ionic interaction of the zinc ion is stronger than that of the sodium or magnesium ion.

Furthermore,  $G'$  and  $G''$  super-master curves<sup>18</sup> (Figure 2) for E/MAA, E/MAA 0.59Zn, E/MAA 0.54Na and E/MAA 0.60Mg were constructed using the horizontal shift of each master curve from the reference master curve of E/MAA at 140°C. The horizontal shift factors ( $a_T^*$ ) for the super-master curve were evaluated as 270 for E/MAA 0.59Zn, 100 for E/MAA 0.54Na and 120 for E/MAA 0.60Mg using the master curve of E/MAA as a reference. The construction of the super-master curve revealed that the branching structure and  $MWD$  are the same among the four samples. In other words, the entanglement molecular weight is not affected by ionic neutralization.

These observations are described by

$$\begin{aligned} G'(270\omega, \text{E/MAA } 0.59\text{Zn}) &= G'(100\omega, \text{E/MAA } 0.54\text{Na}) \\ &= G'(120\omega, \text{E/MAA } 0.60\text{Mg}) \\ &= G'(\omega, \text{E/MAA}) \end{aligned} \quad (1a)$$

and

$$\begin{aligned} G''(270\omega, \text{E/MAA } 0.59\text{Zn}) &= G''(100\omega, \text{E/MAA } 0.54\text{Na}) \\ &= G''(120\omega, \text{E/MAA } 0.60\text{Mg}) \\ &= G''(\omega, \text{E/MAA}) \end{aligned} \quad (1b)$$

where  $\omega$  is the angular frequency. These equations lead us to conclude that the relaxation spectra of E/MAA 0.59Zn, E/MAA 0.54Na and E/MAA 0.60Mg are shifted with respect to the relaxation spectrum of E/MAA by factors of 270, 100 and 120, respectively. According to the tube model of the Doi-Edwards theory<sup>30</sup>, the relaxation times of polymeric chains in tubes are described by the Rouse relaxation time  $\tau_R$  and the longest relaxation time  $\tau_d$

$$\tau_R = \zeta N^2 b^2 / 3\pi^2 k_B T \quad (2a)$$

$$\tau_d = \zeta N^3 b^4 / \pi^2 k_B T a^2 \quad (2b)$$

where  $\zeta$  is the frictional constant of the segment,  $N$  is the number of links in the chain,  $a$  is the average distance between entanglement points,  $b$  is the length of the segment and  $k_B$  is the Boltzmann constant. The polymeric chain motion of ionomer melts can be described as the interchange of ionic groups from one domain to another when polymer chains move. The association and dissociation of ionic bonds in ionomers decrease the polymer chain mobility. According to the tube model<sup>30</sup>, the dynamics of ionomer melts can be explained in terms of the ionic interaction increasing the frictional constant  $\zeta$ . The shift factor  $a_T^*$  corresponds to the degree of increase in friction. Meanwhile, the presence of the ions hardly affects the average distance between entanglement points.

The estimation of the discrete relaxation spectrum of E/MAA from the super-master curves is important in calculating the discrete relaxation spectra of Zn, Na and Mg ionomers using the shift factors  $a_T^*$ . The discrete relaxation spectra are also indispensable for a constitutive analysis of the elongational viscosity. First, we calculated the relaxation spectrum  $H(\tau)$  of E/MAA from  $G'$  and  $G''$  of the super-master curves using the second-order approximation functions of the Tschoegl equations<sup>32</sup>. We determined the longest relaxation time  $\tau_1$  from the point where the dynamic viscosity  $\eta(\omega)$  and the steady shear viscosity  $\eta(\gamma)$  were decreased from zero shear viscosity

**Table 1** The discrete relaxation spectrum of E/MAA

Relaxation time (s)	Relaxation modulus (dyn cm <sup>-2</sup> )
$\tau_1$ 6.32	$1.96 \times 10^2$
$\tau_2$ 2.00	$1.38 \times 10^3$
$\tau_3$ $6.32 \times 10^{-1}$	$5.99 \times 10^3$
$\tau_4$ $2.00 \times 10^{-1}$	$1.84 \times 10^4$
$\tau_5$ $6.32 \times 10^{-2}$	$6.22 \times 10^4$
$\tau_6$ $2.00 \times 10^{-2}$	$1.04 \times 10^5$
$\tau_7$ $6.32 \times 10^{-3}$	$2.42 \times 10^5$
$\tau_8$ $2.00 \times 10^{-3}$	$4.84 \times 10^5$
$\tau_9$ $6.32 \times 10^{-4}$	$7.72 \times 10^5$
$\tau_{10}$ $2.00 \times 10^{-4}$	$1.06 \times 10^6$
$\tau_{11}$ $6.32 \times 10^{-5}$	$1.73 \times 10^6$
$\tau_{12}$ $2.00 \times 10^{-5}$	$2.88 \times 10^6$

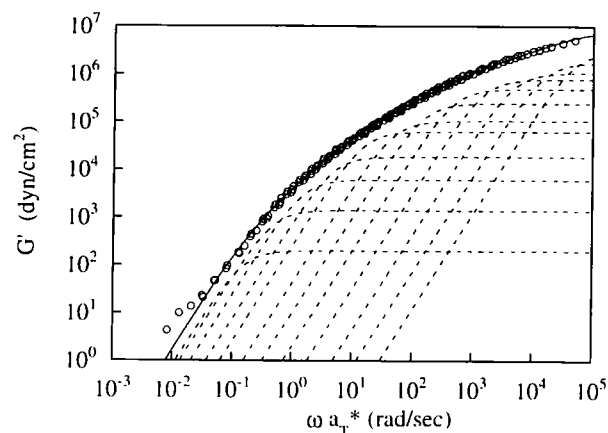


**Figure 3** Comparison between the experimental super-master curve of  $G'$  (open circles) and the prediction (solid line) from the discrete relaxation spectrum of E/MMA. The broken lines represent the predictions from each relaxation modulus corresponding to each relaxation time

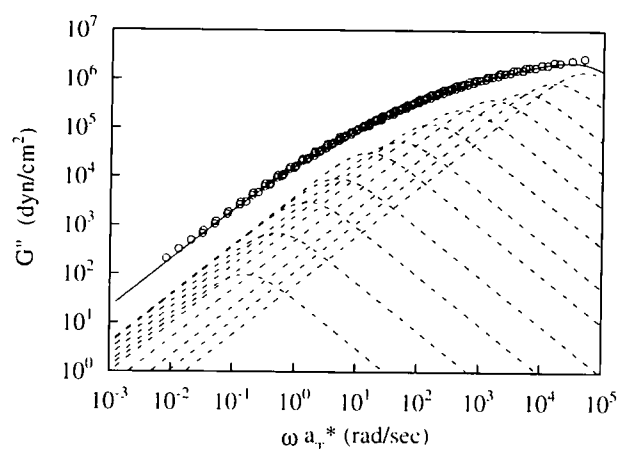


**Figure 4** Comparison between the experimental super-master curve of  $G''$  (open circles) and the prediction (solid line) from the discrete relaxation spectrum of E/MAA. The broken lines represent the predictions from each relaxation modulus corresponding to each relaxation time

( $\tau_1 = \omega_0^{-1} = \gamma_0^{-1}$ )<sup>33</sup>. We estimated the rest of the relaxation times  $\tau_2 - \tau_N$  from the relationship  $\tau_N / \tau_{N-1} = 3.16$ , according to Procedure X<sup>33,34</sup>. The discrete relaxation moduli  $G_N$  were calculated from the areas  $H(\tau)\Delta \ln \tau_N$ . We determined the optimal discrete relaxation spectrum with the help of a trial and error method to adjust  $G'$  and  $G''$  calculated from the discrete spectrum to the experimental  $G'$  and  $G''$  as closely as possible. The obtained discrete relaxation spectrum of E/MAA is listed in Table 1.  $G'$  and  $G''$  were obtained from the spectrum using

$$G'(\omega) = \sum_i G_i \frac{\omega^2 \tau_i^2}{1 + \omega^2 \tau_i^2} \quad (3a)$$

$$G''(\omega) = \sum_i G_i \frac{\omega \tau_i}{1 + \omega^2 \tau_i^2} \quad (3b)$$

Figures 3 and 4 confirm that  $G'$  and  $G''$  calculated from the discrete spectrum agree well with the  $G'$  and  $G''$  from the dynamic shear experiments.

Figures 5–8 show the elongational viscosities of E/MAA, E/MAA 0.59Zn, E/MAA 0.54Na and E/MAA

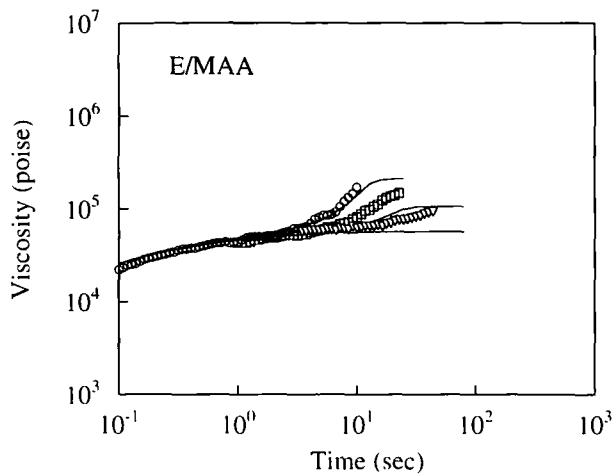


**Figure 5** Uniaxial elongational viscosity ( $1 P = 0.1 \text{ N s m}^{-2}$ ) of E/MAA as a function of time at various constant strain rates ( $\text{s}^{-1}$ ): (○) 0.30; (□) 0.14; (▽) 0.035. The solid lines represent the predictions from the BKZ model with  $\alpha = 200$  and  $\beta = 0.2$ .

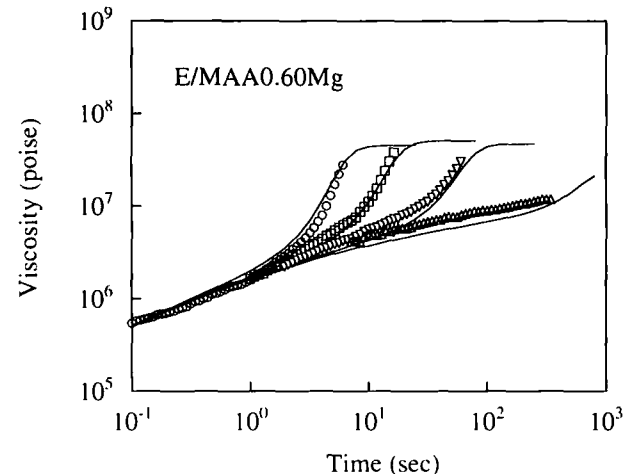


**Figure 8** Uniaxial elongational viscosity of E/MAA 0.60Mg as a function of time at various constant strain rates ( $\text{s}^{-1}$ ): (○) 0.51; (□) 0.18; (▽) 0.043; (△) 0.0044. The solid lines represent the predictions from the BKZ model with  $\alpha = 70$  and  $\beta = 0.2$ .

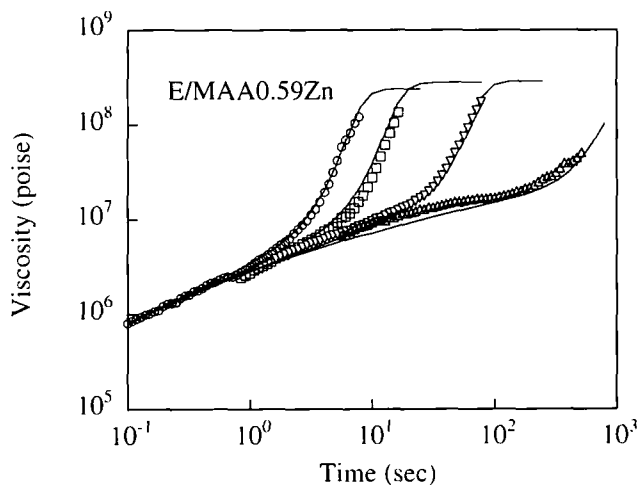


**Figure 6** Uniaxial elongational viscosity of E/MAA 0.59Zn as a function of time at various constant strain rates ( $\text{s}^{-1}$ ): (○) 0.46; (□) 0.22; (▽) 0.046; (△) 0.0042. The solid lines represent the predictions from the BKZ model with  $\alpha = 200$  and  $\beta = 0.2$ .

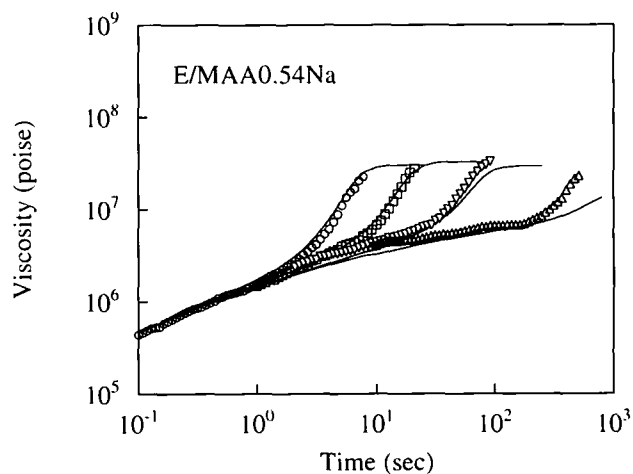


**Figure 7** Uniaxial elongational viscosity of E/MAA 0.54Na as a function of time at various constant strain rates ( $\text{s}^{-1}$ ): (○) 0.46; (□) 0.16; (▽) 0.038; (△) 0.0040. The solid lines represent the predictions from the BKZ model with  $\alpha = 50$  and  $\beta = 0.2$ .

0.60Mg, respectively. The elongational viscosity increases in two steps: the first is a gradual increase in viscosity in the linear region, and the second is a rapid increase in viscosity in the non-linear region. The linear elongational viscosities of the metal (Zn, Na, Mg) salts are larger than that of E/MAA by two orders of magnitude. The linear elongational viscosity of E/MAA 0.59Zn is higher than that of E/MAA 0.54Na and E/MAA 0.60Mg. The order of linear elongational viscosities corresponds to the order of activation energies from dynamic shear measurements. Since the branching structure and  $MWD$  are the same among the four samples from dynamic shear measurements, the degree of increase in linear elongational viscosity is related to the degree of ionic interaction. On the other hand, the linear viscosity differences between E/MAA and its metal salts increase with time. The difference in linear elongational viscosities suggests that long time-scale properties are more influenced by ion neutralization than short time-scale properties. This agrees with the results of other ionomer studies<sup>16,19</sup> which show that long time-scale properties are more affected by ions in steady shear viscosity than short time-scale properties.

Let us explain the relationship between an enhanced frictional constant and a long time-scale property through the relaxation time. The relaxation time linearly depends on the frictional constant (equation (2a) and (2b)). However, the linear elongational property does not linearly depend on the relaxation time. For example, the relaxation time becomes uniformly doubled when the frictional constant becomes uniformly doubled. However, a doubled relaxation time does not lead to a doubled linear elongational property. The reason is that the relationship between the linear elongational property and the relaxation time is described by the BKZ model (equations (4)–(7)), which is given later. The equations indicate that a long time-scale property of the linear elongational viscosity is increased more than a short time-scale property of the linear elongational viscosity (Figures 5–8). Thus, a uniformly enhanced frictional constant implies that the linear elongational property difference between un-ionized and ionized E/MAA

becomes more obvious over a long time-scale than over a short time-scale.

The effect of ionic interaction on the strain rate dependence of the non-linear parameters was examined for E/MAA and its metal salts. The non-linearities of E/MAA were almost independent of strain rate. E/MAA has a wide *MWD* and long-chain branching since it is polymerized in the same way as LDPE. The non-linearities of LDPE with a wide *MWD* are almost independent of strain rate<sup>12</sup>. Hence, the effect of hydrogen bonding on the strain rate dependence of non-linearity is negligible. For metal salts, the non-linearities were also found to be almost independent of strain rate. The results suggest that the effect of ionic bonding on the strain rate dependence of non-linearity is also very small. The non-linear parameters of the four samples are compared in Figure 9. The branching structure and *MWD* are the same among the four samples from dynamic shear measurements. Hence, the results suggest that the non-linearity parameters are enhanced by ion neutralization. E/MAA 0.59Zn shows enhanced non-linearity compared to E/MAA 0.54Na and E/MAA 0.60Mg. The non-linearities of E/MAA 0.54Na and E/MAA 0.60Mg are similar to each other. The order of the degrees of non-linearity is in good agreement with the order of activation energies obtained from dynamic shear measurements. Hence, it was concluded that the degree of ionic interaction determines the degree of non-linearity, as it determines the degree of increase in linear elongational viscosity. It is interesting to note that the zinc ion enhances both the non-linearity and the linear elongational viscosity more than the magnesium ion, even though both ions have double positive electric charges. The question then arises of why the zinc ion shows a larger ionic interaction than the magnesium ion in spite of the same electric charge.

Let us discuss the structural differences among the three ionomers. Several structural studies on E/MAA ionomers in the solid and molten states using dielectric relaxation<sup>35,36</sup>, electron spin resonance (e.s.r.)<sup>37</sup> and small-angle X-ray scattering (SAXS)<sup>19,20</sup> have revealed that ionic groups in ionomers form ionic aggregates, each of which is composed of several ions, when the ion content is low. As the ion content increases, the ionic aggregates

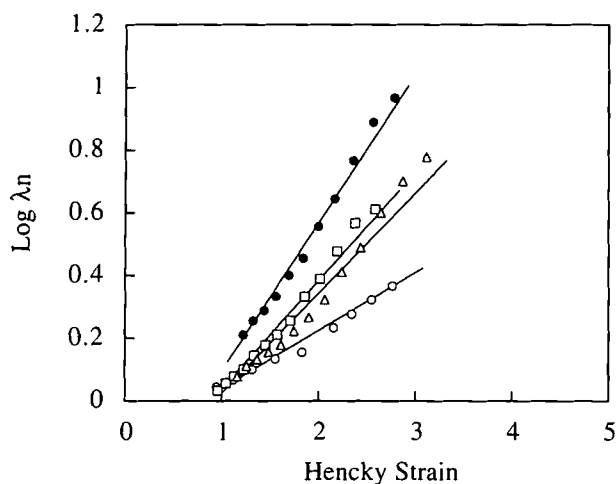


**Figure 9** Non-linear parameters  $\lambda_n$  as a function of Hencky strain for E/MAA (○), E/MAA 0.59Zn (●), E/MAA 0.54Na (□) and E/MAA 0.60Mg (△) at a strain rate of around  $0.45\text{ s}^{-1}$

develop into microphase-separated ionic clusters of the order of  $10\text{ \AA}$  in the hydrophobic domain. The coexistence of hydrogen bonding and ionic bonding up to  $200^\circ\text{C}$  has been confirmed with infra-red spectroscopy<sup>38,39</sup>, SAXS<sup>19,20</sup> and e.s.r.<sup>37</sup>. More importantly, minimum degrees of ion neutralization for cluster formation have been found to be 35% for Na, Mg and Li and 80% for Zn by dynamic mechanical relaxation<sup>40-42</sup> and dielectric relaxation<sup>43</sup> studies. Hence, E/MAA 0.59Zn does not form microphase-separated ionic clusters, but E/MAA 0.54Na and E/MAA 0.60Mg do contain microphase-separated ionic clusters. The different flow properties between zinc and magnesium salts indicate that the cluster formation weakens the ionic interaction.

The effect of ionic interaction was investigated with a BKZ constitutive analysis of elongational viscosity. The separability of the strain dependent function and the time dependent function for E/MAA and its metal salts has been confirmed by recent shear stress relaxation experiments<sup>31</sup>. The following are the BKZ equations<sup>26</sup> employed by us

$$\sigma(t) = \int_{-\infty}^t \mu(t-t') h(I, II) C^{-1}(t-t') dt' \quad (4)$$

$$\mu(t-t') = \sum_i \frac{G_i}{\tau_i} \exp\left[-\frac{(t-t')}{\tau_i}\right] \quad (5)$$

$$h(I, II) = \frac{\alpha}{(\alpha-3) + \beta I + (1-\beta) II} \quad (6)$$

$$C^{-1}(t-t') = \begin{bmatrix} \exp[2\dot{\epsilon}(t-t')] & 0 & 0 \\ 0 & \exp[-\dot{\epsilon}(t-t')] & 0 \\ 0 & 0 & \exp[-\dot{\epsilon}(t-t')] \end{bmatrix} \quad (7)$$

where  $\mu(t-t')$  is the time dependent memory function,  $h(I, II)$  is the strain dependent function, i.e. the damping function, and  $C^{-1}(t-t')$  is the Finger strain tensor for the uniaxial elongational deformation. The discrete relaxation moduli of E/MAA are shown in Table 1, and those of its metal salts were calculated from the E/MAA values using the shift factors  $a_i^*$ . The material parameter  $\alpha$  was estimated using the strain dependent functions from the shear stress relaxation experiments. The strain dependent functions of E/MAA<sup>31</sup> from the experiments were represented by an approximation equation<sup>29,44</sup>

$$h(\gamma) = \frac{1}{1 + a\gamma^2} \quad (8)$$

Equation (6) is a generalized form of equation (8). Equation (9) is derived from equation (6), where  $I = II = 3 + \gamma^2$  for shear deformation

$$h(I, II) = \frac{\alpha}{\alpha - 3 + \beta(3 + \gamma^2) + (1-\beta)(3 + \gamma^2)} = \frac{1}{1 + \alpha^{-1}\gamma^2} \quad (9)$$

Hence, the parameter  $\alpha$  is the reciprocal of the parameter  $a$ . The parameter  $\alpha$  was calculated as 33 for E/MAA. The BKZ equations gave good predictions for the linear

elongational viscosity with this parameter. However, the predictions for non-linearity were not as good. Optimal parameters were determined to fit the non-linear viscosity. Figure 5 shows that values of 200 for  $\alpha$  and 0.2 for  $\beta$  are required to fit the non-linearity at a strain rate of  $0.3 \text{ s}^{-1}$ . The non-linearities at other strain rates were underestimated for E/MAA by the BKZ equations. One way of describing the independent non-linearity of the strain rate using the BKZ equations involves obtaining another long relaxation time spectrum in addition to the already-obtained relaxation spectra, proposed by Koyama and Ishizuka<sup>12</sup>.

The applicability of the superposition principle to  $G'$  and  $G''$  among the four samples suggests that the four samples can be regarded as the same material. The temperature independence of the strain dependent function has been shown experimentally in other studies<sup>25,45,46</sup>. A pair of fixed material parameters ( $\alpha, \beta$ ) should predict the elongational viscosity for one material according to the BKZ equations. The predictability of the elongational viscosities of the metal salts with the material parameters ( $\alpha=200, \beta=0.2$ ) of E/MAA has qualitatively examined. The linear elongational viscosities of the metal salts were adequately predicted with these parameters. The good predictions for the four samples suggest that the effect of ionic interaction in the linear region of elongational deformation is similar to that under dynamic shear deformation. On the other hand, the non-linear viscosities of the Zn salt were predicted with these parameters. However, the parameters overestimated the non-linear viscosities of the Na and Mg ionomers.

Figures 6–8 suggest that smaller values of  $\alpha$  than the value for E/MAA are required to predict the non-linear viscosities of Na and Mg salts with the BKZ equations. (The material parameters  $\alpha$  and  $\beta$  are shown in the captions to these figures.) In other words, the Na and Mg ionomers require larger decreases in the strain dependent functions than E/MAA and the Zn ionomer. This indicates that the effect of Na or Mg bonding is less pronounced in the non-linear region compared to the linear region. This tendency is consistent with the non-linear property determined from shear stress relaxation measurements.

## CONCLUSIONS

The present study of the elongational viscosity of ethylene-based ionomer melts has provided some new findings.

1. According to the tube model and the applicability of the superposition principle to  $G'$  and  $G''$  among E/MAA and its metal salts, the ionic interaction in the linear region can be interpreted as an increase in the frictional constant  $\zeta$  of the polymer segment. The increase in frictional constant corresponds to the shift factor  $a^*$ . The average distance between entanglement points was hardly influenced by the presence of the ion.
2. Both the linear and non-linear elongational viscosities were enhanced by ion neutralization. Zinc increased both viscosities more than sodium and magnesium. The order of viscosities was consistent with the order of activation energies obtained for dynamic shear measurements. It was concluded that the enhancement of both elongational viscosities was caused by ionic interaction. The different viscoelasticities between zinc

and magnesium salts indicated that ionic cluster formation weakens the ionic interaction.

3. The good prediction of linear elongational viscosities from dynamic shear measurements by the BKZ equations revealed that the effect of ionic interaction under linear elongational deformation is similar to that under dynamic shear deformation. On the other hand, the non-linear elongational viscosities of E/MAA and the Zn salt were predicted by the BKZ equations with the same material parameters. However, larger decreases in the strain dependent functions for the Na and Mg salts than those for E/MAA and the Zn salt were required for better prediction, indicating that the ionic interaction of Na or Mg becomes less effective in the non-linear region compared to the linear region under elongational deformation.

## ACKNOWLEDGEMENTS

We express our appreciation to Dr E. Hirasawa, Mr H. Tachino and Mr H. Hara of Mitsui-DuPont Polychemicals for providing the samples and information important to our study.

## REFERENCES

- 1 Munstedt, H. *J. Rheol.* 1980, **24**, 847
- 2 Takahashi, M., Isaki, T., Takigawa, T. and Masuda, T. *J. Rheol.* 1993, **37**, 827
- 3 Li, L., Masuda, T., Takahashi, M. and Ohno, H. *J. Soc. Rheol. Jpn.* 1988, **16**, 117
- 4 Shinohara, M. *J. Soc. Rheol. Jpn.* 1991, **19**, 118
- 5 Schlund, B. and Utracki, L. A. *Polym. Eng. Sci.* 1987, **27**, 380
- 6 Schlund, B. and Utracki, L. A. *Polym. Eng. Sci.* 1987, **27**, 1523
- 7 Laun, H. M. and Munstedt, H. *Rheol. Acta* 1976, **15**, 517
- 8 Meissner, J. *J. Appl. Polym. Sci.* 1972, **16**, 2877
- 9 Zulle, B., Linster, J. J., Meissner, J. and Hurlimann, H. P. *J. Rheol.* 1987, **31**, 583
- 10 Khan, S. A., Prud'homme, R. K. and Larson, R. G. *Rheol. Acta* 1987, **26**, 144
- 11 Koyama, K. and Ishizuka, O. *Polym. Process. Eng.* 1983, **1**, 55
- 12 Koyama, K. and Ishizuka, O. *J. Soc. Rheol. Jpn.* 1985, **13**, 93
- 13 Koyama, K. and Ishizuka, O. *J. Polym. Sci., Polym. Phys. Edn* 1989, **27**, 297
- 14 Ishizuka, O. and Koyama, K. *Polymer* 1980, **21**, 164
- 15 Koyama, K. and Ishizuka, O. *Sen-I Gakkaishi* 1980, **36**, T472
- 16 Sakamoto, K., MacKnight, W. J. and Porter, R. S. *J. Polym. Sci. A-2* 1970, **8**, 277
- 17 Shohamy, E. and Eisenberg, A. *J. Polym. Sci., Polym. Phys. Edn* 1976, **14**, 1211
- 18 Earnest Jr, T. R. and MacKnight, W. J. *J. Polym. Sci., Polym. Phys. Edn* 1978, **16**, 143
- 19 MacKnight, W. J. and Earnest Jr, T. R. *J. Polym. Sci., Macromol. Rev.* 1981, **16**, 41
- 20 Tant, M. R. and Wilkes, G. L. *J. Macromol. Sci., Rev. Macromol. Chem. Phys. C* 1988, **28**, 1
- 21 Connelly, R. W., McConkey, R. C., Noonan, J. M. and Pearson, G. H. *J. Polym. Sci., Polym. Phys. Edn* 1982, **20**, 259
- 22 Bernstein, B., Kearsley, E. A. and Zapas, L. J. *Trans. Soc. Rheol.* 1963, **7**, 391
- 23 Wagner, M. H. *Rheol. Acta* 1976, **15**, 136
- 24 Wagner, M. H. *J. Non-Newtonian Fluid Mech.* 1978, **4**, 39
- 25 Laun, H. M. *Rheol. Acta* 1978, **17**, 1
- 26 Papanastasiou, A. C., Scriven, L. E. and Macosko, C. W. *J. Rheol.* 1983, **27**, 387
- 27 Larson, R. G. 'Constitutive Equations for Polymer Melts and Solutions', AT&T Bell Laboratories, Boston, MA, 1988
- 28 Fukuda, M., Osaki, K. and Kurata, M. *J. Polym. Sci., Polym. Phys. Edn* 1975, **13**, 1563
- 29 Larson, R. G. *J. Rheol.* 1985, **29**, 823
- 30 Doi, M. and Edwards, S. F. 'The Theory of Polymer Dynamics', Oxford University Press, Oxford, 1986

- 31 Takahashi, T., Watanabe, J., Minagawa, K. and Koyama, K. *Rheol. Acta* in press
- 32 Tschoegl, N. W. 'The Theory of Linear Viscoelastic Behavior', Academic Press, New York, 1981
- 33 Takahashi, M., Taku, K. and Masuda, T. *J. Soc. Rheol. Jpn.* 1990, **18**, 18
- 34 Tobolsky, A. V. and Murakami, K. *J. Polym. Sci.* 1959, **40**, 443
- 35 Phillips, P. J. and MacKnight, W. J. *J. Polym. Sci. A-2* 1970, **8**, 727
- 36 Yano, S., Yamashita, H., Matsushita, M., Aoki, K. and Yamauchi, J. *Colloid Polym. Sci.* 1981, **259**, 514
- 37 Takei, M., Tsujita, Y., Shimada, S., Ichihara, H., Enokida, M., Takizawa, A. and Kinoshita, T. *J. Polym. Sci., Polym. Phys. Edn* 1988, **26**, 997
- 38 MacKnight, W. J., McKenna, L. W., Read, B. E. and Stein, R. S. *J. Phys. Chem.* 1968, **72**, 1122
- 39 Blyler Jr, L. L. and Haas, T. W. *J. Appl. Polym. Sci.* 1969, **13**, 2721
- 40 Tadano, K., Hirasawa, E., Yamamoto, H. and Yano, S. *Macromolecules* 1989, **22**, 226
- 41 MacKnight, W. J., Tajiyama, T. and McKenna, L. *Polym. Eng. Sci.* 1968, **8**, 267
- 42 Tachino, H., Hara, H., Hirasawa, E., Kutsumizu, S., Tadano, K. and Yano, S. *Macromolecules* 1993, **26**, 752
- 43 Yano, S., Nagao, N., Hattori, M., Hirasawa, E. and Tadano, K. *Macromolecules* 1992, **25**, 368
- 44 Soskey, P. R. and Winter, H. H. *J. Rheol.* 1984, **28**, 625
- 45 Vinogradov, G. V. and Malkin, A. Y. *J. Polym. Sci. A-2* 1964, **2**, 2357
- 46 Vinogradov, G. V. and Malkin, A. Y. *J. Polym. Sci. A-2* 1966, **4**, 135